NASA TECHNICAL NOTE

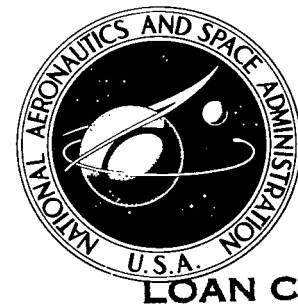

NASA TN D-6765

ARCHED-OUTER-RACE BALL-BEARING ANALYSIS CONSIDERING CENTRIFUGAL FORCES

by Bernard J. Hamrock and William J. Anderson

Lewis Research Center
Cleveland, Ohio 44135

NATIONAL AERONAUTICS AND SPACE ADMINISTRATION • WASHINGTON, D. C. • APRIL 1972

1. Report No.	2. Government Accession No.	3. Recipient's Catalog No.
NASA TN D-6765		

4. Title and Subtitle

ARCHED-OUTER-RACE BALL-BEARING ANALYSIS CONSIDERING CENTRIFUGAL FORCES

5. Report Date: April 1972

6. Performing Organization Code

7. Author(s)

Bernard J. Hamrock and William J. Anderson

8. Performing Organization Report No.: E-6767

9. Performing Organization Name and Address

Lewis Research Center
National Aeronautics and Space Administration
Cleveland, Ohio 44135

10. Work Unit No.: 114-03

11. Contract or Grant No.

13. Type of Report and Period Covered: Technical Note

12. Sponsoring Agency Name and Address

National Aeronautics and Space Administration
Washington, D.C. 20546

14. Sponsoring Agency Code

15. Supplementary Notes

16. Abstract

A first-order thrust load analysis that considers centrifugal forces but which neglects gyroscopics, elastohydrodynamics, and thermal effects was performed. The analysis was applied to a 150-mm-bore angular-contact ball bearing. Fatigue life, contact loads, and contact angles are shown for conventional and arched bearings. The results indicate that an arched bearing is highly desirable for high-speed applications. In particular, at an applied load of 4448 N (1000 lb) and a DN value of 3 million (20 000 rpm), the arched bearing shows an improvement in life of 306 percent over that of a conventional bearing.

17. Key Words (Suggested by Author(s))

Arched ball bearing
High-speed ball bearing

18. Distribution Statement

Unclassified - unlimited

19. Security Classif. (of this report)	20. Security Classif. (of this page)	21. No. of Pages	22. Price*
Unclassified	Unclassified	34	$3.00

* For sale by the National Technical Information Service, Springfield, Virginia 22151

ARCHED-OUTER-RACE BALL-BEARING ANALYSIS CONSIDERING CENTRIFUGAL FORCES

by Bernard J. Hamrock and William J. Anderson

Lewis Research Center

SUMMARY

A thrust load analysis of an arched-outer-race ball bearing that considers centrifugal forces but that neglects gyroscopics, elastohydrodynamics, and thermal effects was performed. Elliptic integrals were evaluated by using the Landen transformation. A one-point iteration method was used in evaluating the load-deflection constant. A Newton-Raphson method of iteration was used in evaluating the axial displacement and the radial and axial projection of the distance between the ball center and the outer-raceway groove curvature center. Fatigue life evaluations were made. The similar analysis of a conventional bearing can be directly obtained from the arched-bearing analysis by simply letting the amount of arching be zero (g = 0) and not considering equations related to the unloaded half of the outer race.

The analysis was applied to a 150-millimeter-bore, angular-contact ball bearing. Results for life, contact loads, and contact angles are shown for a conventional bearing (g = 0) and several arched bearings (g = 0.127 mm (0.005 in.), 0.254 mm (0.010 in.), . . ., and 0.762 mm (0.030 in.)). The results indicate that an arched bearing is highly desirable for high-speed applications. In particular, for a DN value of 3 million (20 000 rpm) and an applied axial load of 4448 newtons (1000 lb), an arched bearing shows an improvement in life of 306 percent over that of a conventional bearing. At 4.2 million DN (28 000 rpm), the corresponding improvement is 340 percent. It was also found that the arched bearing does not offer the advantages at low speeds that it does at high speeds.

INTRODUCTION

Aircraft gas turbine engine rotor bearings currently operate in the speed range from 1.5 to 2 million DN (bearing bore in mm times shaft speed in rpm). It is esti-

mated that engine designs of the next decade will require bearings to operate at DN values of 3 million or more (ref. 1). In this DN range, analyses (refs. 2 and 3) predict a prohibitive reduction in bearing fatigue life due to the high centrifugal forces developed between the rolling elements and the outer race.

Several approaches to the high-speed-bearing problem have been suggested and are being developed. One approach is to reduce ball mass through the use of thin-wall spherically hollow balls (ref. 4) or drilled balls (refs. 5 to 7). Theory indicates that significant improvements in bearing fatigue life can be obtained at DN values of 3 million and above with a 50 percent or greater weight removal from the balls. Flexure failures have occurred with both hollow and drilled balls after short running times, however, so that both of these concepts must still be considered highly experimental.

Hybrid bearings consisting of a combination ball and fluid film bearing constitute a second approach. The parallel hybrid bearing (ref. 8), in which the fluid film bearing and ball bearing share the system load with both operating at full speed, can be used to improve high-speed-ball-bearing life. However, the effectiveness of the parallel hybrid bearing diminishes at high speeds because it does not attenuate centrifugal effects in the ball bearing. The series hybrid bearing (refs. 9 and 10), in which a fluid film bearing and a ball bearing both carry full system load while each operates at part speed, is theoretically the most effective approach to extending high-speed-ball-bearing life. This concept, too, is still quite experimental. Mechanical complexity is a problem, and effects on shaft stiffness and rotor dynamics must be evaluated.

Initial experiments with an arched-outer-race ball bearing (ref. 11) indicated that this design operated with lower torque than a conventional angular-contact bearing. The experiments of reference 11 were conducted at DN values up to about 1 million. In light of the successful experiments of reference 11, the arched-outer-race ball bearing seemed to be a promising high-speed-bearing concept because of its ability to share the centrifugal loading at two outer-race contacts per ball.

The objective of the work described in this report was to conduct a fatigue life analysis of the arched-outer-race ball bearing and to compare the fatigue life of this bearing with that of a conventional bearing at various combinations of thrust load and speed. A first-order thrust load analysis, in which gyroscopic, elastohydrodynamic and thermal effects are neglected, is reported.

SYMBOLS

A distance between raceway groove curvature centers

$\mathscr{A}$ right-side-outer-race curvature center

a semimajor axis of projected contact ellipse

B $f_o + f_i - 1 = A/D$

$\mathscr{B}$ ball center initially

b semiminor axis of projected contact ellipse

$\mathscr{C}$ initial position, inner-raceway groove curvature center

c function of axial displacement defined in eq. (53)

D ball diameter

$\mathscr{D}$ left-side-outer-race curvature center

d raceway diameter

d_m pitch diameter

E percent improvement of arch bearing (g = 0.005) over that of conventional bearing (g = 0), $\left(\frac{L|_{g=0.005} - L|_{g=0}}{L|_{g=0}}\right)100$

$\mathscr{E}$ elliptical integral of second kind

F curvature difference

F_a axially applied load

F_c centrifugal force

$\mathscr{F}$ elliptic integral of first kind

f r/D

G, H functions of V and W defined by eqs. (27) and (28)

$\mathscr{G}$ inner-race contact, initially

g amount of arching, or width of material removed from outer race of conventional bearing

$\mathfrak{H}$ outer-race contact, initially

h distance from top of arch to top of ball when bearing is in radial contact position

$\mathscr{I}$ inner-race contact, finally

J function of k defined by eq. (45)

$\mathscr{J}$ right-outer-race contact, finally

K load-deflection constant

$\mathscr{K}$ left-outer-race contact, finally

k a/b

L life, hr

$\mathscr{L}$ ball center, finally

M defined by eq. (63)

$\mathscr{M}$ final position, inner-raceway groove curvature center

m ball mass

N defined by eq. (64)

$\mathscr{N}$ tip of arch

n rotational speed

P basic dynamic capacity of raceway contact

P_d bearing diametral clearance

P_e free end play

Q ball normal load

r raceway groove curvature radius

S distance between inner- and outer-raceway groove curvature center loci

S_d diametral play

T τ_o/σ_{max}

T_1 $\left(\tau_o/\sigma_{max}\right)_{k=1}$

U surface velocity

u number of stress cycles per revolution

V radial projection of distance between ball center and outer-raceway groove curvature center

W axial projection of distance between ball center and outer-raceway groove curvature center

x defined in eq. (31)

Y diameter of ball track

y defined in eq. (32)

Z number of balls

z_o depth of maximum shear stress

α radial contact angle

β axial contact angle

γ $D \cos \beta / \bar{d}_m$

Δ distance between raceway groove curvature center and final position of ball center

δ contact deformation

δ_a axial displacement

δ^* defined by eq. (50)

ζ ratio of depth of maximum shear stress to semiminor axis, z_o/b

ζ_1 $(\zeta)_{k=1}$

η defined by eq. (9)

λ modulus of elasticity

ξ Poisson's ratio

ρ curvature sum

σ_{max} maximum normal stress

τ_o maximum orthogonal subsurface shear stress

φ auxiliary angle

Ω defined in eq. (74)

ω_m orbital speed of ball

Subscripts:

B ball

i inner raceway

n iteration

o outer raceway

ol left outer raceway

or right outer raceway

x x-direction

y y-direction

z z-direction

Superscript:

$-$ final position

ARCHED-BEARING GEOMETRY

Figure 1 shows how the arched outer race is made. A conventional outer race is shown in figure 1(a) with a race radius of r_o. Also shown in figure 1(a) is the portion of the conventional outer race that is removed in forming an arched outer race. Figure 1(b) shows the arched outer race with the portion of length g removed. Note that there are now two outer-race radius centers separated by a distance g.

Figure 2 shows the arched bearing while in a noncontacting position. Here the pitch diameter d_m, diametral clearance P_d, diametral play S_d, and raceway diameters d_i and d_o are defined. The diametral play is the total amount of radial movement allowed in the bearing. Furthermore, the diametral clearance is the diametral play plus two times the distance from the bottom of the ball to the tip of the arch when the bearing is in a radial contact position.

Figure 3 shows the arched bearing in a radial contact position. Instead of contacting at one point at the bottom of the outer raceway, the ball contacts at two points separated by an angle 2α. From figure 3 the radial contact angle α can be written as

$$\alpha = \sin^{-1}\left(\frac{g}{2r_o - D}\right) \tag{1}$$

A distance which needs to be formulated is the distance from the tip of the arch to the bottom of the ball when the ball and raceway are in the radial contact position as shown in figure 3. This distance is defined as h. From figure 3(b) and the Pythagorian theorem the following can be written:

$$r_o^2 = \left(r_o - \frac{D}{2}\right)^2 \sin^2\alpha + \left[h + \frac{D}{2} + \left(r_o - \frac{D}{2}\right)\cos\alpha\right]^2$$

Solving for h results in

$$h = -\frac{D}{2} - \left(r_o - \frac{D}{2}\right)\cos\alpha + \frac{1}{2}\left[D(4r_o - D) + (2r_o - D)^2\cos^2\alpha\right]^{1/2} \tag{2}$$

Note that as one might expect as $\alpha \to 0^o$, $h \to 0$. With h known, a number of conventional bearing parameters can be formulated from figures 2 and 3. The outer-raceway diameter may be written as

$$d_o = d_i + P_d + 2D \tag{3}$$

where

$$P_d = S_d + 2h \tag{4}$$

From equations (3) and (4) the diametral play can be written as

$$S_d = d_o - d_i - 2D - 2h \tag{5}$$

The pitch diameter d_m from figure 2 can be expressed as

$$d_m = d_i + \frac{S_d}{2} + D \tag{6}$$

Figure 4 shows the arched ball bearing while in the axial contact position. Note that the ball is in the top position. From this figure the distance between the center of curvature of the inner and right outer race can be written as

$$A = r_o + r_i - D$$

With $f_o = r_o/D$ and $f_i = r_i/D$ this equation becomes

$$A = BD \tag{7}$$

where

$$B = f_o + f_i - 1 \tag{8}$$

From figure 4(b) the following equation can be written:

$$r_o^2 = \left(\frac{g}{2}\right)^2 + (r_o - \eta)^2$$

Solving for η gives

$$\eta = r_o - \sqrt{r_o^2 - \left(\frac{g}{2}\right)^2} \tag{9}$$

With η known, the contact angle can be expressed as

$$\cos \beta = \frac{A - \frac{P_d}{2} - \eta}{A}$$

or

$$\beta = \cos^{-1}\left(\frac{A - \frac{P_d}{2} - \eta}{A}\right) \tag{10}$$

The end play of an arched bearing is

$$P_e = 2A \sin \beta - g \tag{11}$$

ANALYSIS

Contact Geometry

From the experimental work of Haines and Edmonds (ref. 11) it is observed that the arched bearing will initially operate with two-point contact at the lower speeds and then with three-point contact at higher speeds when the centrifugal forces become significant. When centrifugal force acts on the ball, the inner- and outer-raceway contact angles are dissimilar; therefore, the lines of action between raceway groove curvature radius centers become discontinuous, as shown in figure 5. In this figure the right- and left-outer-raceway groove curvature centers $\mathscr{A}$ and $\mathscr{D}$ are fixed in space, and the inner-raceway groove curvature center $\mathscr{C}$ moves axially relative to these fixed centers.

When the general approach of reference 12 is followed and figure 5 is used, the distance between the fixed right- and left-outer-raceway groove curvature centers $\mathscr{A}$ and $\mathscr{D}$ and the final position of the ball center $\mathscr{L}$ can be written as

$$\Delta_{o\ell} = r_o - \frac{D}{2} + \delta_{o\ell} = (f_o - 0.5)D + \delta_{o\ell} \tag{12}$$

$$\Delta_{or} = (f_o - 0.5)D + \delta_{or} \tag{13}$$

where $\delta_{o\ell}$ is the normal contact deformation at the left-outer-raceway center, and δ_{or}

is the normal contact deformation at the right-outer-raceway center. Similarly, the distance between the final inner-raceway groove curvature center $\mathscr{M}$ and the final position of the ball center $\mathscr{L}$ is

$$\Delta_i = (f_i - 0.5)D + \delta_i \tag{14}$$

where δ_i is the normal contact deformation at the inner-raceway center.

The axial distance between the final position of the inner- and right-outer-raceway groove curvature center is

$$S_x = A \sin \beta + \delta_a \tag{15}$$

where δ_a is the axial displacement. The radial distance between the final position of the inner-raceway groove curvature center and the right- or left-outer-raceway groove curvature center is

$$S_z = A \cos \beta \tag{16}$$

From figure 5 and equations (12) to (16) the following can be written:

$$\cos \beta_{ol} = \frac{V}{(f_o - 0.5)D + \delta_{ol}} \tag{17}$$

$$\sin \beta_{ol} = \frac{g - W}{(f_o - 0.5)D + \delta_{ol}} \tag{18}$$

$$\cos \beta_{or} = \frac{V}{(f_o - 0.5)D + \delta_{or}} \tag{19}$$

$$\sin \beta_{or} = \frac{W}{(f_o - 0.5)D + \delta_{or}} \tag{20}$$

$$\cos \beta_i = \frac{A \cos \beta - V}{(f_i - 0.5)D + \delta_i} \tag{21}$$

$$\sin \beta_i = \frac{A \sin \beta + \delta_a - W}{(f_i - 0.5)D + \delta_i} \tag{22}$$

Using the Pythagorean theorem and regrouping terms result in

$$\delta_{ol} = \sqrt{V^2 + (g - W)^2} - D(f_o - 0.5) \tag{23}$$

$$\delta_{or} = \sqrt{V^2 + W^2} - D(f_o - 0.5) \tag{24}$$

$$\delta_i = \sqrt{(A \cos \beta - V)^2 + (A \sin \beta + \delta_a - W)^2} - D(f_i - 0.5) \tag{25}$$

The normal loads shown in figure 6 are related to the normal contact deformation in the following way:

$$Q = K\delta^{1.5} \tag{26}$$

With proper subscripting of i, ol, and or this equation could represent the normal loads of the inner ring Q_i, left outer ring Q_{ol}, or right outer ring Q_{or}. From figure 6 the equilibrium equations of the forces in the horizontal and vertical directions are

$$Q_i \sin \beta_i + Q_{ol} \sin \beta_{ol} - Q_{or} \sin \beta_{or} = 0$$

$$Q_i \cos \beta_i - Q_{ol} \cos \beta_{ol} - Q_{or} \cos \beta_{or} + F_c = 0$$

Substituting equations (15) to (22) and (26) into these equations gives

$$\frac{K_i \delta_i^{1.5}(S_x - W)}{(f_i - 0.5)D + \delta_i} - \frac{K_{or} \delta_{or}^{1.5} W}{(f_o - 0.5)D + \delta_{or}} + \frac{K_{ol} \delta_{ol}^{1.5}(g - W)}{(f_o - 0.5)D + \delta_{ol}} = 0 = G(V, W) \tag{27}$$

$$\frac{K_i \delta_i^{1.5}(S_z - V)}{(f_i - 0.5)D + \delta_i} - \frac{K_{or} \delta_{or}^{1.5} V}{(f_o - 0.5)D + \delta_{or}} - \frac{K_{ol} \delta_{ol}^{1.5} V}{(f_o - 0.5)D + \delta_{ol}} + F_c = 0 = H(V, W) \tag{28}$$

Before equations (27) and (28) are solved for V and W, the expressions for the load-deflection constants, the centrifugal force, and the axial contact displacement must be developed.

Centrifugal Force

From figure 7 the following two right triangles can be drawn:

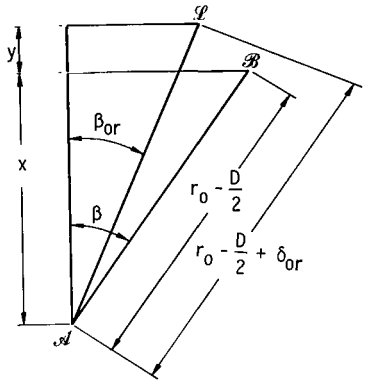

Solving for x and y, we get

$$x = \left(r_o - \frac{D}{2}\right)\cos\beta \tag{29}$$

$$y = \left(r_o - \frac{D}{2} + \delta_{or}\right)\cos\beta_{or} - \left(r_o - \frac{D}{2}\right)\cos\beta \tag{30}$$

Note that in figure 7 the unbarred values represent initial location, and the barred values represent final location when the centrifugal forces have acted on the ball. From figure 7 the pitch diameter when the centrifugal force acts on the ball is $\overline{dm} = dm + 2y$ or

$$\overline{d}_m = d_m + 2\left(r_o - \frac{D}{2} + \delta_{or}\right)\cos\beta_{or} - 2\left(r_o - \frac{D}{2}\right)\cos\beta \tag{31}$$

Also from figure 7 the contact diameters can be written

$$\overline{Y}_i = (1 - \gamma_i)\,\overline{d}_m \tag{32}$$

$$\overline{Y}_{o\ell} = (1 + \gamma_{o\ell})\,\overline{d}_m \tag{33}$$

$$\overline{Y}_{or} = (1 + \gamma_{or})\,\overline{d}_m \tag{34}$$

where

$$\left.\begin{aligned} \gamma_i &= \frac{D \cos \beta_i}{\bar{d}_m} \\ \gamma_{ol} &= \frac{D \cos \beta_{ol}}{\bar{d}_m} \\ \gamma_{or} &= \frac{D \cos \beta_{or}}{\bar{d}_m} \end{aligned}\right\} \tag{35}$$

The surface velocities at the contacts and contact diameters are represented vectorially by

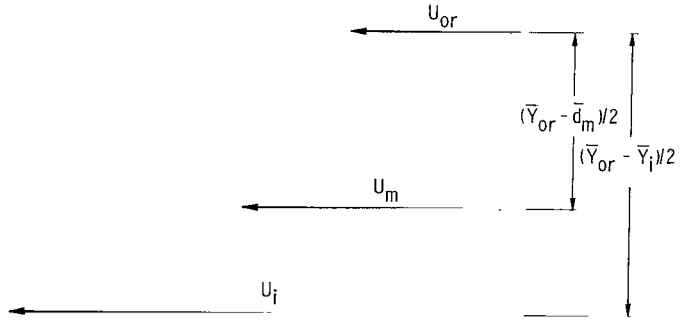

From this representation the following equation which neglects spin, can be written:

$$\frac{U_i - U_{or}}{U_m - U_{or}} = \frac{\dfrac{\bar{Y}_{or} - \bar{Y}_i}{2}}{\dfrac{\bar{Y}_{or} - \bar{d}_m}{2}}$$

or

$$U_m = U_{or} + (U_i - U_{or})\left(\frac{\bar{Y}_{or} - \bar{d}_m}{\bar{Y}_{or} - \bar{Y}_i}\right) \tag{36}$$

But

$$U = \omega \frac{Y}{2} = \frac{\pi n Y}{60}$$

Therefore,

$$\omega_m = \frac{\pi}{30\,\bar{d}_m}\left[n_{or}\bar{Y}_{or} + (n_i\bar{Y}_i - n_{or}\bar{Y}_{or})\left(\frac{\bar{Y}_{or} - \bar{d}_m}{\bar{Y}_{or} - \bar{Y}_i}\right)\right] \tag{37}$$

Finally, the equation for the centrifugal force is

$$F_c = \frac{1}{2}\, m\, \bar{d}_m\, \omega_m^2 \tag{38}$$

Where m is the ball mass.

Load-Deflection Constants

The equations for the curvature sum and differences can be obtained from reference 12:

$$\rho_i = \frac{1}{D}\left(4 - \frac{1}{f_i} + \frac{2\gamma_i}{1 - \gamma_i}\right) \tag{39}$$

$$\rho_{ol} = \frac{1}{D}\left(4 - \frac{1}{f_o} - \frac{2\gamma_{ol}}{1 + \gamma_{ol}}\right) \tag{40}$$

$$\rho_{or} = \frac{1}{D}\left(4 - \frac{1}{f_o} - \frac{2\gamma_{or}}{1 + \gamma_{or}}\right) \tag{41}$$

$$F_i = \frac{\dfrac{1}{f_i} + \dfrac{2\gamma_i}{1 - \gamma_i}}{4 - \dfrac{1}{f_i} + \dfrac{2\gamma_i}{1 - \gamma_i}} \tag{42}$$

$$F_{ol} = \frac{\frac{1}{f_o} - \frac{2\gamma_{ol}}{1 + \gamma_{ol}}}{4 - \frac{1}{f_o} - \frac{2\gamma_{ol}}{1 + \gamma_{ol}}} \tag{43}$$

$$F_{or} = \frac{\frac{1}{f_o} - \frac{2\gamma_{or}}{1 + \gamma_{or}}}{4 - \frac{1}{f_o} - \frac{2\gamma_{or}}{1 + \gamma_{or}}} \tag{44}$$

From reference 12 auxiliary equations (45) to (47), relating the curvature difference and the elliptic integrals of the first and second kind, can be written:

$$k = \sqrt{\frac{2\mathscr{F} - \mathscr{E}(1 + F)}{\mathscr{E}(1 - F)}} = J(k) \tag{45}$$

$$\mathscr{F} = \int_0^{\pi/2} \left[1 - \left(1 - \frac{1}{k^2}\right)\sin^2 \varphi\right]^{-1/2} d\varphi \tag{46}$$

$$\mathscr{E} = \int_0^{\pi/2} \left[1 - \left(1 - \frac{1}{k^2}\right)\sin^2 \varphi\right]^{1/2} d\varphi \tag{47}$$

where

$$k = \frac{a}{b}$$

in which a and b are the semimajor and semiminor axes, respectively, of the projected elliptical area of contact. A one-point iteration method will be used in evaluating equation (45), where

$$k_{n+1} = J(k_n) \tag{48}$$

From reference 12 the following can be written:

$$\delta = \delta^* \left[\frac{3Q}{2\rho} \left(\frac{1 - \xi_B^2}{\lambda_B} + \frac{1 - \xi^2}{\lambda} \right) \right]^{2/3} \left(\frac{\rho}{2} \right) \tag{49}$$

where

$$\delta^* = \frac{2\mathscr{F}}{\pi} \left(\frac{\pi}{2k^2 \mathscr{E}} \right)^{1/3} \tag{50}$$

From equations (26) and (49) the following can be written:

$$K = \frac{(2)^{5/2} (\delta^*)^{-3/2} (\rho)^{-1/2}}{3 \left(\frac{1 - \xi_B^2}{\lambda_B} + \frac{1 - \xi^2}{\lambda} \right)} \tag{51}$$

With proper subscripting of i, oℓ, and or in equations (45) to (51) three sets of corresponding equations can be obtained for the inner race, the outer left race, and the outer right race.

The elliptic integrals (eqs. (46) and (47)) were evaluated by using a method described by Bulirsch (ref. 13). In this reference a short algorithm is described which makes it possible to compute these integrals very rapidly. The method of evaluation is the Landen transformation. This method, coupled with using a one-point iteration method in evaluating k_i, $k_{o\ell}$, and k_{or} proved to be a fast method as compared to presently used formulations. For example, compared to a Ralston integration scheme the method used was 26 times faster.

Axial Displacement

Thrust ball bearings subjected to centric thrust load have the load distributed equally among the balls. Hence,

$$Q_i = \frac{F_a}{Z \sin \beta_i} \tag{52}$$

where Z is the number of balls. Substituting equation (26) into equation (52) gives

$$0 = -\frac{F_a}{ZK_i} + \delta_i^{3/2} \sin \beta_i = C(\delta_a) \tag{53}$$

A Newton-Raphson iteration method will be used to evaluate δ_a in equation (53). The derivative of $C(\delta_a)$ with respect to δ_a when equation (22) and (25) are used, gives

$$\frac{\partial C(\delta_a)}{\partial \delta_a} = \frac{\delta_i^{1/2}}{D(f_i - 0.5) + \delta_i} \left\{ \delta_i + \frac{\sin^2 \beta_i}{2} \left[\delta_i + 3D(f_i - 0.5) \right] \right\} \tag{54}$$

Therefore, the Newton-Raphson iteration equation is written as

$$\delta_{a,n+1} = \delta_{a,n} - \frac{C(\delta_{a,n})}{\frac{\partial C(\delta_{a,n})}{\partial \delta_a}} \tag{55}$$

Therefore, for a given value of V and W and using equations developed thus far, one is able to use equation (55) to find δ_a while satisfying equation (53).

Computer Evaluation

Having derived expressions for the centrifugal force F_c, the load deflection constants K_i, $K_{o\ell}$, and K_{or}, and the axial displacement δ_a in equations (38), (51), and (55), we can now return to solving for V and W in equations (27) and (28). The method to be used to solve this system of nonlinear equations is the Newton-Raphson iteration method, which can be found in most numerical analysis books (e.g., ref. 14). When this method is used, the following equations can be written:

$$V_{n+1} = V_n - \frac{1}{\Omega} \left(G \frac{\partial H}{\partial W} - H \frac{\partial G}{\partial W} \right)_{V=V_n,\, W=W_n} \tag{56}$$

$$W_{n+1} = W_n - \frac{1}{\Omega} \left(H \frac{\partial G}{\partial V} - G \frac{\partial H}{\partial V} \right)_{V=V_n,\, W=W_n} \tag{57}$$

where

$$\Omega = \left(\frac{\partial G}{\partial V}\frac{\partial H}{\partial W} - \frac{\partial G}{\partial W}\frac{\partial H}{\partial V}\right)_{V=V_n,\, W=W_n} \tag{58}$$

$$\frac{\partial G}{\partial V} = -N_i(A\cos\beta - V)(A\sin\beta + \delta_a - W) + N_{o\ell}V(g - W) - N_{or}VW \tag{59}$$

$$\frac{\partial G}{\partial W} = -N_i(A\sin\beta + \delta_a - W)^2 - N_{o\ell}(g - W)^2 - N_{or}W^2 - M_i - M_{o\ell} - M_{or} \tag{60}$$

$$\frac{\partial H}{\partial V} = -N_i(A\cos\beta - V)^2 - V^2(N_{o\ell} + N_{or}) - M_i - M_{o\ell} - M_{or} \tag{61}$$

$$\frac{\partial H}{\partial W} = -N_i(A\cos\beta - V)(A\sin\beta + \delta_a - W) + N_{o\ell}V(g - W) - N_{or}VW \tag{62}$$

where

$$M = \frac{K\delta^{3/2}}{\delta + D(f - 0.5)} \tag{63}$$

$$N = \frac{K\delta^{1/2}[\delta + 3D(f - 0.5)]}{2[\delta + D(f - 0.5)]^3} \tag{64}$$

Therefore, with equations (56) and (57) we are able to find values of V and W which satisfy the system of equations. With V and W known and given equations (17) to (26), the contact loads Q_i, $Q_{o\ell}$, and Q_{or} and angles β_i, $\beta_{o\ell}$, and β_{or} can be evaluated.

Derivation of Fatigue Life

From the weakest link theory, on which the Weibull equation is based, we get the relation between life of an assembly (the bearing) and its components (the inner and outer rings):

$$\frac{1}{L} = \frac{12n_i}{1\times10^6}\left[\left(\frac{1}{L_i}\right)^{10/9} + \left(\frac{1}{L_{ol}}\right)^{10/9} + \left(\frac{1}{L_{or}}\right)^{10/9}\right]^{9/10} \tag{65}$$

In this equation life L is expressed in hours. A material improvement factor of 5 has been assumed; however, no adjustment factors for reliability or operating conditions have been added. For point contact

$$L = (P/Q)^3 \tag{66}$$

Therefore, equation (65) becomes

$$L = \frac{1\times10^6}{12n_i}\frac{1}{\left[\left(\frac{Q_i}{P_i}\right)^{10/3} + \left(\frac{Q_{ol}}{P_{ol}}\right)^{10/3} + \left(\frac{Q_{or}}{P_{or}}\right)^{10/3}\right]^{0.9}} \tag{67}$$

The contact loads are defined by equation (26). From Lundberg and Palmgren (ref. 15) the following can be written:

$$P = 84\,000\,D^{1.8}\left(\frac{T_1}{T}\right)^{3.1}\left(\frac{\zeta}{\zeta_1}\right)^{0.4}\left(\frac{\partial\mathscr{E}}{\pi D\rho}\right)^{2.1}(k)^{0.7}\left(\frac{D}{d}\right)^{0.3}u^{-1/3} \tag{68}$$

With proper subscripting of i, ol, and or this equation can represent the dynamic loads of the inner ring P_i, the left outer ring P_{ol}, and the right outer ring P_{or}.

Variations of the T and ζ functions with curvature over the range from 0.52 to 0.54 are 2.3 and 0.8 percent, respectively. The variation of the product of these functions over the curvature range from 0.52 to 0.54 is less than 2 percent. Therefore, for the range just described, the products of the T and ζ functions can be considered a constant in equation (68), or

$$\left(\frac{T_1}{T}\right)^{3.1}\left(\frac{\zeta}{\zeta_1}\right)^{0.4} = 0.718 \tag{69}$$

The number of stress cycles per revolution for each contact is, to a good approximation,

$$u_i = \frac{Z}{2}(1 + \gamma_i) \tag{70}$$

$$u_{o\ell} = \frac{Z}{2}(1 - \gamma_{o\ell}) \tag{71}$$

$$u_{or} = \frac{Z}{2}(1 - \gamma_{or}) \tag{72}$$

Substituting equations (69) to (72) into equation (68), one can obtain the dynamic capacity at the inner ring and left and right outer rings as

$$P_i = \frac{60\ 312}{d_i^{0.3}}\left(\frac{2\mathscr{E}_i}{\pi\rho_i}\right)^{2.1} k_i^{0.7}\left[\frac{Z}{2}(1 + \gamma_i)\right]^{-1/3} \tag{73}$$

$$P_{o\ell} = \frac{60\ 312}{d_o^{0.3}}\left(\frac{2\mathscr{E}_{o\ell}}{\pi\rho_{o\ell}}\right)^{2.1} k_{o\ell}^{0.7}\left[\frac{Z}{2}(1 - \gamma_{o\ell})\right]^{-1/3} \tag{74}$$

$$P_{or} = \frac{60\ 312}{d_o^{0.3}}\left(\frac{2\mathscr{E}_{or}}{\pi\rho_{or}}\right)^{2.1} k_{or}^{0.7}\left[\frac{Z}{2}(1 - \gamma_{or})\right]^{-1/3} \tag{75}$$

Therefore, from equations (26), (73) to (75), and (67) the life in hours of the bearing can be obtained. The equations for a conventional bearing can be directly obtained from the arched-bearing analysis by simply letting the amount of arching be zero (g = 0) and not considering equations related to the left outer race.

DISCUSSION OF RESULTS

Comparison of Arched and Conventional Bearings

A conventional 150-millimeter ball thrust bearing was used for the computer evaluation. Bearing parameters and results such as life, contact loads, and contact angles for various speeds and axial loads are shown in table I for the conventional bearing. Then calculations were made for the arched bearing (fig. 1(b)). The diametral play S_d (fig. 2) was set fixed at 0.2499 millimeter (0.0098 in.) for all the results presented. In an arched bearing the free contact angle becomes larger than that of the conventional bearing even though the diametral play is held constant. The greater the amount of

arching (the larger the g), the higher the free contact angle. Also some of the other bearing geometry parameters were changed by changing the amount of arching. Tables II to VII show the effect of the amount of arching (g = 0.127 mm (0.005 in.), 0.254 mm (0.010 in.), . . ., 0.762 mm (0.030 in.)) on life, contact loads, and contact angles for various speeds and axial loads.

The following observations can be made from the results in tables I to VII:

(1) For high speeds ($n_i \geq 20\ 000$ rpm) there is a substantial increase in life for an arched bearing compared to a conventional bearing.

(2) At high speeds and light loads the longest life is obtained with a g of 0.127 millimeter (0.005 in.).

(3) There is less advantage in using an arched bearing at high loads ($F_a \geq 13\ 345$ N (3000 lb)).

(4) For low speeds the arched bearing does not offer the advantages that it does for high speeds.

(5) At low speeds and a small amount of arching the arched bearing operates at a two-point contact.

(6) As the applied load F_a increases, the speed for initial three-point contact increases.

(7) As the amount of arching is increased, the speed where the arched bearing has initial three-point contact decreases. The arched bearing operates with three-point contact whenever Q_{ol} is not zero.

(8) Even small contact loads ($Q_{ol} \approx 100$ N (22.48 lb)) at the left outer race help to improve the life significantly over a conventional bearing.

Figure 8 shows the percent improvement in fatigue life for an arched bearing (g = 0.127 mm (0.005 in.)) over that of a conventional bearing for axial loads of 4448, 13 345, and 22 241 newtons (1000, 3000, and 5000 lb). The ordinate E of figure 8 is defined by the following relation:

$$E = \left(\frac{L\big|_{g=0.005} - L\big|_{g=0}}{L\big|_{g=0}} \right) 100 \tag{76}$$

The figure shows that the improvement over the conventional bearing is significant for high-speed applications. For example, at $n_i = 28\ 000$ rpm and $F_a = 4448$ newtons (1000 lb), the improvement in life for an arched bearing (g = 0.127 mm (0.005 in.)) is 340 percent. As the applied load F_a increases, the advantage of the arched bearing becomes less significant.

Bearing Size Effects

The use of bearing sizes other than the 150-millimeter-bore diameter for comparing the performance of arched and conventional bearings would yield somewhat different but qualitatively similar results. The relative importance of centrifugal effects in bearings of different sizes can be determined by comparing the ratio of D^3n^2 to the dynamic capacity. The factor D^3n^2 is proportional to centrifugal force, and dynamic capacity is a measure of the load capacity of the bearing. For extra-light series angular contact ball bearings operating at 3 million DN the following data are obtained:

Bore diameter, mm	D^3n^2	Dynamic capacity	D^3n^2 dynamic capacity
50	1.46×10^8	5 010	2.91×10^4
100	1.6	14 400	1.11
150	2.68	31 210	.86
200	4.38	54 790	.80

It is seen that centrifugal effects are relatively more severe in small bearings when DN is kept constant. Thus, life improvement of the arched bearing will be greater than that shown for bearings smaller than 150-millimeter bore and somewhat less for larger bearings.

SUMMARY OF RESULTS

A first-order thrust load analysis of an arched bearing which considers centrifugal forces but which neglects gyroscopics, elastohydrodynamics, and thermal effects was performed. Elliptic integrals were evaluated by using the Landen transformation. A one-point iteration method was used in evaluating the load-deflection constant. A Newton-Raphson method of iteration was used in evaluating the axial displacement and the radial and axial projection of the distance between the ball center and the outer-raceway groove curvature center. Fatigue life evaluations were made. The similar analysis of a conventional bearing can be obtained directly from the arched-bearing analysis by simply letting the amount of arching be zero ($g = 0$) and not considering equations related to the unloaded half of the outer race.

Computer solutions were obtained for a 150-millimeter-bore ball bearing. The amount of arching investigated was from zero to g equal to 0.76 millimeter (0.030 in.). The following results were obtained:

1. The arched bearing shows significant improvements in fatigue life over a conventional bearing, especially at high speeds. In particular, at an axial load of 4448 newtons (1000 lb) the life improvement is 306 percent at 3 million DN and 340 percent at 4.2 million DN.

2. There is an optimal value of g to produce maximum life for a given value of diametral play and thrust load. For the particular bearing investigated life improvement was greatest at a thrust load of 4448 newtons (1000 lb) when g was 0.127 millimeter (0.005 in.).

3. For low speeds the arched bearing does not offer the advantages that it does for high speeds.

Lewis Research Center,
National Aeronautics and Space Administration,
Cleveland, Ohio, February 10, 1972,
114-03.

REFERENCES

1. Brown, Paul F.: Bearings and Dampers for Advanced Jet Engines. Paper 700318, SAE, Apr. 1970.

2. Jones, A. B.: Ball Motion and Sliding Friction in Ball Bearings. J. Basic Eng., vol. 81, no. 1, Mar. 1959, pp. 1-12.

3. Harris, T. A.: An Analytical Method to Predict Skidding in Thrust-Loaded, Angular-Contact Ball Bearings. J. Lub. Tech., vol. 93, no. 1, Jan. 1971, pp. 17-24.

4. Coe, Harold H.; Parker, Richard J.; and Scibbe, Herbert W.: Evaluation of Electron-Beam Welded Hollow Balls for High-Speed Ball Bearings. J. Lub. Tech., vol. 93, no. 1, Jan. 1971, pp. 47-59.

5. Coe, Harold H.; Scibbe, Herbert W.; and Anderson, William J.: Evaluation of Cylindrically Hollow (Drilled) Balls in Ball Bearings at DN Values to 2.1 Million. NASA TN D-7007, 1971.

6. Holmes, P. W.: Evaluation of Drilled-Ball Bearings at DN Values to Three Million. I - Variable Oil Flow Tests. NASA CR-2004, 1972.

7. Holmes, P. W.: Evaluation of Drilled-Ball Bearings at DN Values to Three Million. II - Experimental Skid Study and Endurance Tests. NASA CR-2005, 1972.

8. Wilcock, D. F.; and Winn, L. W.: The Hybrid Boost Bearing - A Method of Obtaining Long Life in Rolling Contact Bearing Applications. J. Lub. Tech., vol. 92, no. 3, July 1970, pp. 406-414.

9. Anderson, William J.; Fleming, David P.; and Parker, Richard J.: The Series Hybrid Bearing: A New High Speed Bearing Concept. Paper 71-LUB-15, ASME, Oct. 1971.

10. Nypan, Lester J.; Hamrock, Bernard J.; Scibbe, Herbert W.; and Anderson, William J.: Optimization of Conical Hydrostatic Bearing for Minimum Friction. Paper 71-LUB-19, ASME, Oct. 1971.

11. Haines, D. J.; and Edmonds, M. J.: A New Design of Angular Contact Ball Bearing. Proc. Inst. Mech. Eng., vol. 185, 1970-1971, pp. 382-393.

12. Harris, Tedric A.: Rolling Bearing Analysis. John Wiley & Sons, Inc., 1966.

13. Bulirsch, Roland: Numerical Calculation of Elliptic Integrals and Elliptic Functions. Numerische Mathematik, vol. 7, 1965, pp. 78-90.

14. Moursund, David G.; and Duris, Charles S.: Elementary Theory and Application of Numerical Analysis. McGraw-Hill Book Co., Inc., 1967.

15. Lundberg, G.; and Palmgren, A.: Dynamic Capacity of Rolling Bearings. Acta Polytech., Mech. Eng. Ser., vol. 1, no. 3, issue 7, 1947.

TABLE I. - LIFE, CONTACT LOADS, AND CONTACT ANGLES FOR CONVENTIONAL BEARING (ZERO ARCHING) AT CONTACT ANGLE OF 25° AND VARIOUS SPEEDS AND AXIAL APPLIED FORCES

[Inner-raceway groove curvature, 0.54; outer-raceway groove curvature, 0.52; pitch diameter, 187.55 mm (7.3838 in.); ball diameter, 22.23 mm (0.8750 in.); diametral play, 0.2499 mm (0.0098 in.); 22 balls.]

	Rotational speed of inner raceway, n_i, rpm						
	4000	8000	12 000	16 000	20 000	24 000	28 000
Axially applied load, F_a, 4448 N (1000 lb)							
Life, L, hr	342 291	84 727	11 478	1955	450	130	45
Inner-raceway load, Q_i, N	426.3	389.5	376.0	368.1	361.2	354.5	347.9
Right-outer-raceway load, Q_{or}, N	570.1	1037	1911	3167	4809	6849	9302
Inner-raceway contact angle, β_i, deg	28.31	31.28	32.53	33.32	34.04	34.77	35.53
Right-outer-raceway contact angle, β_{or}, deg	20.77	11.25	6.075	3.662	2.411	1.693	1.246
Axially applied load, F_a, 13 345 N (3000 lb)							
Life, L, hr	13 432	6996	3163	1007	302	99	37
Inner-raceway load, Q_i, N	1297	1208	1138	1098	1072	1050	1030
Right-outer-raceway load, Q_{or}, N	1433	1799	2579	3796	5427	7466	9924
Inner-raceway contact angle, β_i, deg	27.88	30.14	32.20	33.53	34.48	35.29	36.08
Right-outer-raceway contact angle, β_{or}, deg	25.03	19.70	13.60	9.192	6.417	4.659	3.503
Axially applied load, F_a, 22 241 N (5000 lb)							
Life, L, hr	3060	1649	1016	500	199	76	30
Inner-raceway load, Q_i, N	2137	2030	1915	1833	1778	1737	1702
Right-outer-raceway load, Q_{or}, N	2271	2598	3293	4440	6035	8060	10 515
Inner-raceway contact angle, β_i, deg	28.23	29.87	31.86	33.47	34.65	35.60	36.44
Right-outer-raceway contact angle, β_{or}, deg	26.43	22.90	17.88	13.16	9.642	7.204	5.516

TABLE II. - LIFE, CONTACT LOADS, AND CONTACT ANGLES FOR BEARING WITH 0.127-MILLIMETER (0.005-IN.) ARCHING AT CONTACT ANGLE OF 25.46° AND VARIOUS SPEEDS AND AXIAL APPLIED FORCES

[Inner-raceway groove curvature, 0.54; outer raceway groove curvature, 0.52; pitch diameter, 187.55 mm (7.3838 in.); ball diameter, 22.23 mm (0.8750 in.); diametral play, 0.2499 mm (0.0098 in.); 22 balls.]

	Rotational speed of inner raceway, n_i, rpm						
	4000	8000	12 000	16 000	20 000	24 000	28 000
Axially applied load, F_a, 4448 N (1000 lb)							
Life, L, hr	358 866	89 881	26 299	6804	1825	560	198
Inner-raceway load, Q_i, N	419.5	384.2	379.3	375.0	370.5	366.0	361.4
Left-outer-raceway load, Q_{ol}, N	0	20.01	503.4	1178	2031	3068	4292
Right-outer-raceway load, Q_{or}, N	563.4	1015	1404	1969	2727	3682	4837
Inner-raceway contact angle, β_i, deg	31.41	31.76	32.21	32.63	33.07	33.53	34.01
Left-outer-raceway contact angle, β_{ol}, deg	0	4.645	5.761	6.318	6.655	6.867	6.996
Right-outer-raceway contact angle, β_{or}, deg	10.62	11.59	10.37	9.698	9.236	8.892	8.621
Axially applied load, F_a, 13 345 N (3000 lb)							
Life, L, hr	14 036	7288	3411	1752	817	348	146
Inner-raceway load, Q_i, N	1279	1180	1127	1110	1095	1082	1069
Left-outer-raceway load, Q_{ol}, N	0	0	80.51	784.4	1701	2802	4087
Right-outer-raceway load, Q_{or}, N	1415	1783	2492	3006	3691	4578	5675
Inner-raceway contact angle, β_i, deg	28.31	30.63	32.57	33.14	33.63	34.10	34.58
Left-outer-raceway contact angle, β_{ol}, deg	0	0	1.879	3.393	4.339	4.998	5.467
Right-outer-raceway contact angle, β_{or}, deg	25.38	19.89	14.15	12.54	11.49	10.71	10.11
Axially applied load, F_a, 22 241 N (5000 lb)							
Life, L, hr	3188	1717	1051	622	372	204	103
Inner-raceway load, Q_i, N	2109	2003	1890	1836	1809	1785	1763
Left-outer-raceway load, Q_{ol}, N	0	0	0	48.37	1423	2567	3898
Right-outer-raceway load, Q_{or}, N	2243	2571	3272	3955	4595	5428	6474
Inner-raceway contact angle, β_i, deg	28.64	30.32	32.34	33.41	33.98	34.49	34.99
Left-outer-raceway contact angle, β_{ol}, deg	0	0	0	.9138	2.310	3.315	4.060
Right-outer-raceway contact angle, β_{or}, deg	26.79	23.15	18.00	14.93	13.44	12.33	11.46

TABLE III. - LIFE, CONTACT LOADS, AND CONTACT ANGLES FOR BEARING WITH 0.254-MILLIMETER (0.010-IN.) ARCHING AT CONTACT ANGLE OF 26.82° AND VARIOUS SPEEDS AND AXIAL APPLIED FORCES

[Inner-raceway groove curvature, 0.54; outer raceway groove curvature, 0.52; pitch diameter, 187.55 mm (7.3838 in.); ball diameter, 22.23 mm (0.8750 in.); diametral play, 0.2499 mm (0.0098 in.); 22 balls.]

	Rotational speed of inner raceway, n_i, rpm						
	4000	8000	12 000	16 000	20 000	24 000	28 000
Axially applied load, F_a, 4448 N (1000 lb)							
Life, L, hr	411 173	128 403	31 701	7084	1803	545	192
Inner-raceway load, Q_i, N	400.5	382.2	378.4	374.2	369.8	365.2	360.6
Left-outer-raceway load, Q_{ol}, N	0	194.2	644.8	1279	2101	3113	4320
Right-outer-raceway load, Q_{or}, N	545.1	847.7	1276	1886	2681	3667	4848
Inner-raceway contact angle, β_i, deg	31.46	31.94	32.30	32.70	33.14	33.61	34.11
Left-outer-raceway contact angle, β_{ol}, deg	0	15.40	15.53	15.55	15.53	15.47	15.38
Right-outer-raceway contact angle, β_{or}, deg	17.71	17.41	17.07	16.81	16.57	16.36	16.15
Axially applied load, F_a, 13 345 N (3000 lb)							
Life, L, hr	15 944	8191	4210	2011	855	345	142
Inner-raceway load, Q_i, N	1228	1141	1115	1103	1091	1078	1065
Left-outer-raceway load, Q_{ol}, N	0	0	371.4	1020	1861	2896	4128
Right-outer-raceway load, Q_{or}, N	1363	1738	2212	2800	3571	4533	5691
Inner-raceway contact angle, β_i, deg	29.60	32.10	32.96	33.36	33.78	34.23	34.71
Left-outer-raceway contact angle, β_{ol}, deg	0	0	14.12	14.38	14.52	14.60	14.62
Right-outer-raceway contact angle, β_{or}, deg	26.42	20.42	18.37	17.88	17.49	17.14	16.84
Axially applied load, F_a, 22 241 N (5000 lb)							
Life, L, hr	3591	1931	1180	707	396	204	100
Inner-raceway load, Q_i, N	2031	1926	1837	1816	1796	1776	1755
Left-outer-raceway load, Q_{ol}, N	0	0	132.2	778.2	1631	2682	3934
Right-outer-raceway load, Q_{or}, N	2164	2496	3106	3683	4434	5373	6509
Inner-raceway contact angle, β_i, deg	29.86	31.67	33.40	33.84	34.26	34.70	35.17
Left-outer-raceway contact angle, β_{ol}, deg	0	0	12.84	13.31	13.60	13.78	13.90
Right-outer-raceway contact angle, β_{or}, deg	27.85	23.89	19.56	18.85	18.33	17.88	17.49

TABLE IV. - LIFE, CONTACT LOADS, AND CONTACT ANGLES FOR BEARING WITH 0.381-MILLIMETER (0.015-IN.) ARCHING AT CONTACT ANGLE OF 29.06° AND VARIOUS SPEEDS AND AXIAL APPLIED FORCES

[Inner-raceway groove curvature, 0.54; outer raceway groove curvature, 0.52; pitch diameter, 187.55 mm (7.3838 in.); ball diameter, 22.23 mm (0.8750 in.); diametral play, 0.2499 mm (0.0098 in.); 22 balls.]

	Rotational speed of inner raceway, n_i, rpm						
	4000	8000	12 000	16 000	20 000	24 000	28 000
Axially applied load, F_a, 4448 N (1000 lb)							
Life, L, hr	479 904	149 602	33 736	7027	1739	521	183
Inner-raceway load, Q_i, N	384.5	381.4	377.5	373.2	368.6	363.9	359.0
Left-outer-raceway load, $Q_{o\ell}$, N	37.71	301.3	745.3	1373	2189	3197	4404
Right-outer-raceway load, Q_{or}, N	501.5	761.1	1201	1822	2631	3632	4830
Inner-raceway contact angle, β_i, deg	31.72	32.02	32.38	32.80	33.26	33.75	34.28
Left-outer-raceway contact angle, $\beta_{o\ell}$, deg	24.60	24.62	24.54	24.41	24.25	24.06	23.85
Right-outer-raceway contact angle, β_{or}, deg	25.77	25.49	25.24	24.99	24.75	24.50	24.24
Axially applied load, F_a, 13 345 N (3000 lb)							
Life, L, hr	19 476	9317	4829	2218	888	343	138
Inner-raceway load, Q_i, N	1152	1121	1110	1099	1087	1074	1060
Left-outer-raceway load, $Q_{o\ell}$, N	0	198.1	642.1	1273	2094	3109	4324
Right-outer-raceway load, Q_{or}, N	1287	1561	1993	2608	3409	4403	5594
Inner-raceway contact angle, β_i, deg	31.77	32.78	33.12	33.50	33.93	34.40	34.90
Left-outer-raceway contact angle, $\beta_{o\ell}$, deg	0	23.81	23.84	23.80	23.71	23.58	23.42
Right-outer-raceway contact angle, β_{or}, deg	28.13	26.09	25.75	25.44	25.14	24.84	24.55
Axially applied load, F_a, 22 241 N (5000 lb)							
Life, L, hr	4335	2254	1342	796	431	212	100
Inner-raceway load, Q_i, N	1913	1840	1824	1806	1787	1767	1746
Left-outer-raceway load, $Q_{o\ell}$, N	0	96.79	536.2	1167	1991	3011	4232
Right-outer-raceway load, Q_{or}, N	2045	2339	2768	3376	4170	5155	6340
Inner-raceway contact angle, β_i, deg	31.90	33.32	33.67	34.04	34.45	34.90	35.38
Left-outer-raceway contact angle, $\beta_{o\ell}$, deg	0	23.12	23.23	23.25	23.21	23.13	23.01
Right-outer-raceway contact angle, β_{or}, deg	29.63	26.63	26.21	25.84	25.50	25.18	24.85

TABLE V. - LIFE, CONTACT LOADS, AND CONTACT ANGLES FOR BEARING WITH 0.508-MILLIMETER (0.020-IN.) ARCHING AT CONTACT ANGLE OF 32.16° AND VARIOUS SPEEDS AND AXIAL APPLIED FORCES

[Inner-raceway groove curvature, 0.54; outer raceway groove curvature, 0.52; pitch diameter, 187.55 mm (7.3838 in.); ball diameter, 22.23 mm (0.8750 in.); diametral play, 0.2499 mm (0.0098 in.); 22 balls.]

	Rotational speed of inner raceway, n_i, rpm						
	4000	8000	12 000	16 000	20 000	24 000	28 000
Axially applied load, F_a, 4448 N (1000 lb)							
Life, L, hr	501 596	153 552	32 663	6613	1623	485	170
Inner-raceway load, Q_i, N	383.5	380.3	376.2	371.6	366.6	361.5	356.3
Left-outer-raceway load, Q_{ol}, N	110.1	372.6	815.4	1443	2260	3272	4486
Right-outer-raceway load, Q_{or}, N	462.8	725.2	1167	1793	2609	3620	4831
Inner-raceway contact angle, β_i, deg	31.81	32.11	32.50	32.96	33.46	34.00	34.57
Left-outer-raceway contact angle, β_{ol}, deg	34.26	34.14	33.94	33.70	33.42	33.11	32.79
Right-outer-raceway contact angle, β_{or}, deg	34.83	34.59	34.31	34.01	33.69	33.35	33.00
Axially applied load, F_a, 13 345 N (3000 lb)							
Life, L, hr	21 476	9806	5032	2233	860	324	129
Inner-raceway load, Q_i, N	1123	1115	1105	1093	1080	1066	1052
Left-outer-raceway load, Q_{ol}, N	138.3	398.5	839.4	1466	2283	3296	4511
Right-outer-raceway load, Q_{or}, N	1191	1450	1889	2512	3326	4334	5544
Inner-raceway contact angle, β_i, deg	32.70	32.95	33.29	33.70	34.16	34.67	35.20
Left-outer-raceway contact angle, β_{ol}, deg	33.67	33.61	33.47	33.28	33.05	32.78	32.49
Right-outer-raceway contact angle, β_{or}, deg	35.00	34.76	34.47	34.15	33.82	33.48	33.12
Axially applied load, F_a, 22 241 N (5000 lb)							
Life, L, hr	4966	2381	1415	827	434	207	95
Inner-raceway load, Q_i, N	1839	1828	1813	1795	1775	1754	1732
Left-outer-raceway load, Q_{ol}, N	153.1	410.9	849.6	1474	2290	3303	4520
Right-outer-raceway load, Q_{or}, N	1901	2159	2595	3216	4025	5031	6239
Inner-raceway contact angle, β_i, deg	33.35	33.58	33.90	34.28	34.71	35.19	35.70
Left-outer-raceway contact angle, β_{ol}, deg	33.21	33.17	33.07	32.91	32.71	32.47	32.20
Right-outer-raceway contact angle, β_{or}, deg	35.15	34.91	34.61	34.29	33.95	33.60	33.23

TABLE VI. - LIFE, CONTACT LOADS, AND CONTACT ANGLES FOR BEARING WITH 0.635-MILLIMETER (0.025-IN.) ARCHING AT CONTACT ANGLE OF 36.22° AND VARIOUS SPEEDS AND AXIAL APPLIED FORCES

[Inner-raceway groove curvature, 0.54; outer raceway groove curvature, 0.52; pitch diameter, 187.55 mm (7.3838 in.); ball diameter, 22.23 mm (.8750 in.); diametral play, 0.2499 mm (0.0098 in.); 22 balls.]

	Rotational speed of inner raceway, n_i, rpm						
	4000	8000	12 000	16 000	20 000	24 000	28 000
Axially applied load, F_a, 4448 N (1000 lb)							
Life, L, hr	498 260	144 853	29 572	5971	1472	441	154
Inner-raceway load, Q_i, N	381.9	378.5	373.9	368.8	363.2	357.6	351.9
Left-outer-raceway load, Q_{ol}, N	175.4	435.0	874.3	1499	2317	3333	4556
Right-outer-raceway load, Q_{or}, N	459.5	719.4	1159	1785	2603	3620	4842
Inner-raceway contact angle, β_i, deg	31.96	32.28	32.73	33.25	33.82	34.43	35.08
Left-outer-raceway contact angle, β_{ol}, deg	44.94	44.72	44.41	44.03	43.61	43.16	42.68
Right-outer-raceway contact angle, β_{or}, deg	45.24	44.97	44.61	44.21	43.77	43.30	42.80
Axially applied load, F_a, 13 345 N (3000 lb)							
Life, L, hr	21 776	9812	4880	2081	782	292	116
Inner-raceway load, Q_i, N	1115	1107	1096	1083	1069	1054	1038
Left-outer-raceway load, Q_{ol}, N	322.5	579.7	1016	1637	2450	3464	4685
Right-outer-raceway load, Q_{or}, N	1175	1433	1870	2493	3308	4323	5545
Inner-raceway contact angle, β_i, deg	32.97	33.23	33.60	34.05	34.57	35.14	35.75
Left-outer-raceway contact angle, β_{ol}, deg	44.35	44.23	43.98	43.65	43.27	42.86	42.40
Right-outer-raceway contact angle, β_{or}, deg	45.08	44.85	44.52	44.14	43.71	43.26	42.77
Axially applied load, F_a, 22 241 N (5000 lb)							
Life, L, hr	5083	2420	1415	803	408	189	86
Inner-raceway load, Q_i, N	1821	1811	1796	1777	1755	1733	1709
Left-outer-raceway load, Q_{ol}, N	445.2	700.6	1134	1752	2562	3573	4792
Right-outer-raceway load, Q_{or}, N	1868	2124	2560	3180	3992	5006	6225
Inner-raceway contact angle, β_i, deg	33.72	33.94	34.27	34.68	35.16	35.70	36.28
Left-outer-raceway contact angle, β_{ol}, deg	43.97	43.83	43.61	43.32	42.97	42.58	42.15
Right-outer-raceway contact angle, β_{or}, deg	44.97	44.76	44.45	44.09	43.67	43.23	42.75

TABLE VII. - LIFE, CONTACT LOADS, AND CONTACT ANGLES FOR BEARING WITH 0.762-MILLIMETER (0.030-IN.) ARCHING AT CONTACT ANGLE OF 41.87° AND VARIOUS SPEEDS AND AXIAL APPLIED FORCES

[Inner-raceway groove curvature, 0.54; outer raceway groove curvature, 0.52; pitch diameter, 187.55 mm (7.3838 in.); ball diameter, 22.23 mm (0.8750 in.); diametral play, 0.2499 mm (0.0098 in.); 22 balls.]

	Rotational speed of inner raceway, n_i, rpm						
	4000	8000	12 000	16 000	20 000	24 000	28 000
Axially applied load, F_a, 4448 N (1000 lb)							
Life, L, hr	451 172	120 028	24 692	5205	1315	397	139
Inner-raceway load, Q_i, N	378.2	374.2	368.8	362.6	355.9	349.2	342.5
Left-outer-raceway load, Q_{ol}, N	267.5	514.0	935.2	1542	2345	3355	4584
Right-outer-raceway load, Q_{or}, N	505.3	752.5	1175	1782	2586	3598	4828
Inner-raceway contact angle, β_i, deg	32.31	32.70	33.25	33.89	34.61	35.38	36.19
Left-outer-raceway contact angle, β_{ol}, deg	58.01	57.66	57.17	56.59	55.93	55.23	54.48
Right-outer-raceway contact angle, β_{or}, deg	58.15	57.79	57.28	56.68	56.02	55.30	54.55
Axially applied load, F_a, 13 345 N (3000 lb)							
Life, L, hr	20 985	9073	4257	1754	660	249	100
Inner-raceway load, Q_i, N	1096	1088	1076	1061	1045	1028	1010
Left-outer-raceway load, Q_{ol}, N	575.7	818.8	1234	1832	2626	3627	4848
Right-outer-raceway load, Q_{or}, N	1292	1537	1954	2555	3352	4357	5582
Inner-raceway contact angle, β_i, deg	33.60	33.88	34.32	34.86	35.49	36.18	36.93
Left-outer-raceway contact angle, β_{ol}, deg	57.22	56.96	56.57	56.06	55.48	54.83	54.13
Right-outer-raceway contact angle, β_{or}, deg	57.55	57.27	56.85	56.32	55.72	55.05	54.34
Axially applied load, F_a, 22 241 N (5000 lb)							
Life, L, hr	5023	2335	1310	710	349	160	73
Inner-raceway load, Q_i, N	1784	1774	1757	1736	1713	1687	1660
Left-outer-raceway load, Q_{ol}, N	836.7	1078	1490	2083	2871	3864	5078
Right-outer-raceway load, Q_{or}, N	2035	2279	2694	3292	4084	5083	6303
Inner-raceway contact angle, β_i, deg	34.51	34.75	35.13	35.61	36.18	36.82	37.52
Left-outer-raceway contact angle, β_{ol}, deg	56.64	56.42	56.07	55.62	55.08	54.48	53.82
Right-outer-raceway contact angle, β_{or}, deg	57.13	56.89	56.51	56.03	55.47	54.84	54.16

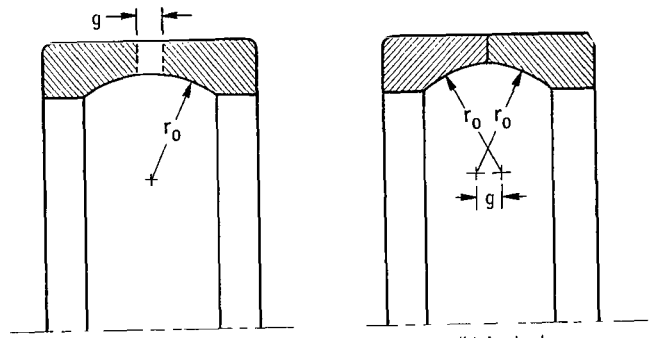

(a) Conventional. (b) Arched.

Figure 1. - Bearing outer race geometries.

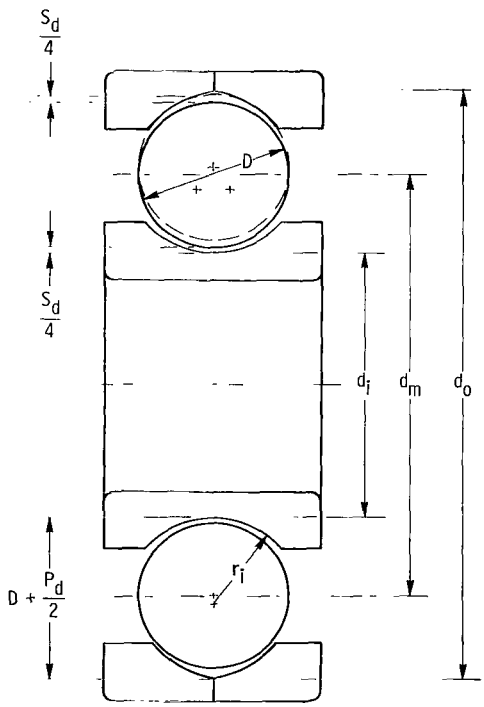

Figure 2. - Arched ball bearing in noncontacting position.

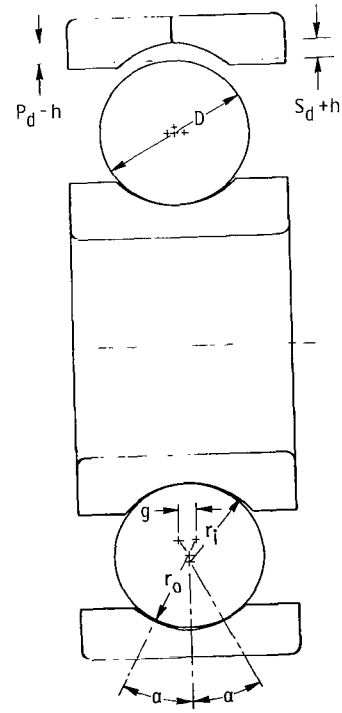

(a) Radial contact position.

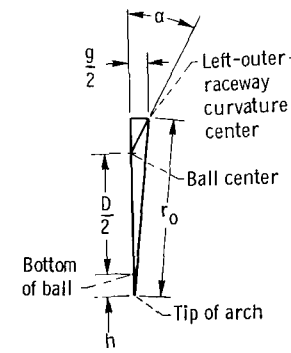

(b) Details of contact.

Figure 3. - Arched ball bearing radially loaded.

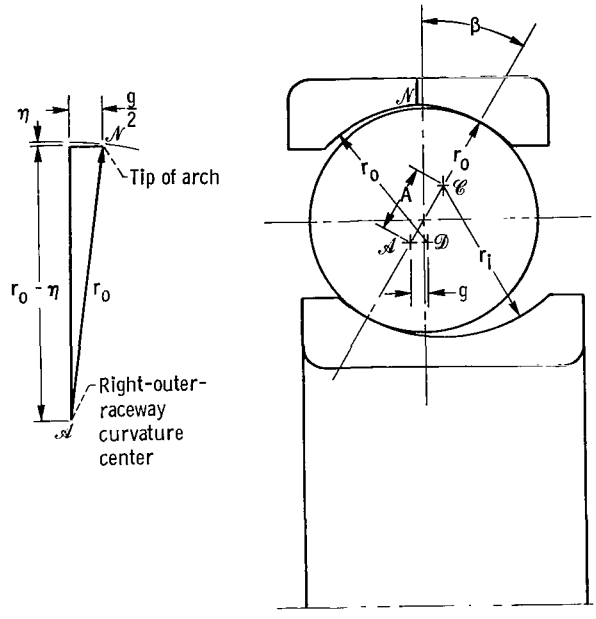

(a) Details of contact. (b) Axial contact position of top ball.

Figure 4. - Arched ball bearing axially loaded.

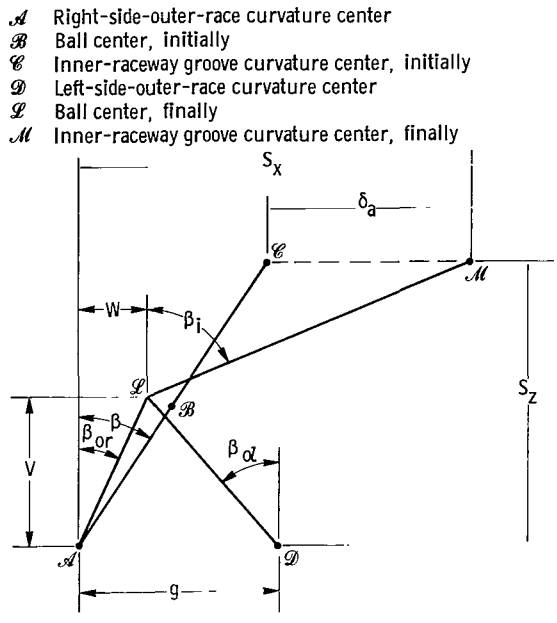

- $\mathscr{A}$ Right-side-outer-race curvature center
- $\mathscr{B}$ Ball center, initially
- $\mathscr{C}$ Inner-raceway groove curvature center, initially
- $\mathscr{D}$ Left-side-outer-race curvature center
- $\mathscr{L}$ Ball center, finally
- $\mathscr{M}$ Inner-raceway groove curvature center, finally

Figure 5. - Position of ball center and raceway groove curvature centers with and without centrifugal force acting on the ball. Points shown for ball in top position, with bearing loaded axially.

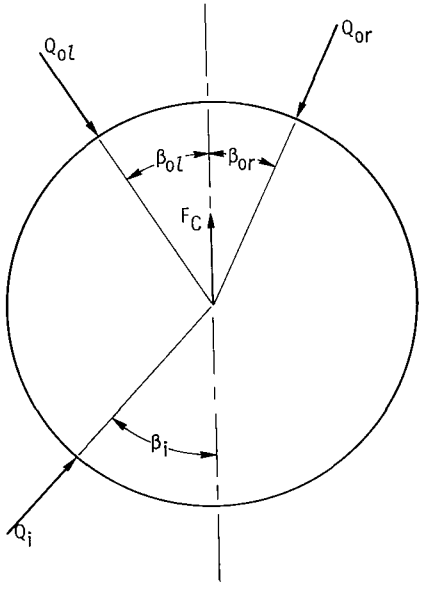

Figure 6. - Normal ball loading. Ball in top position; bearing axially loaded.

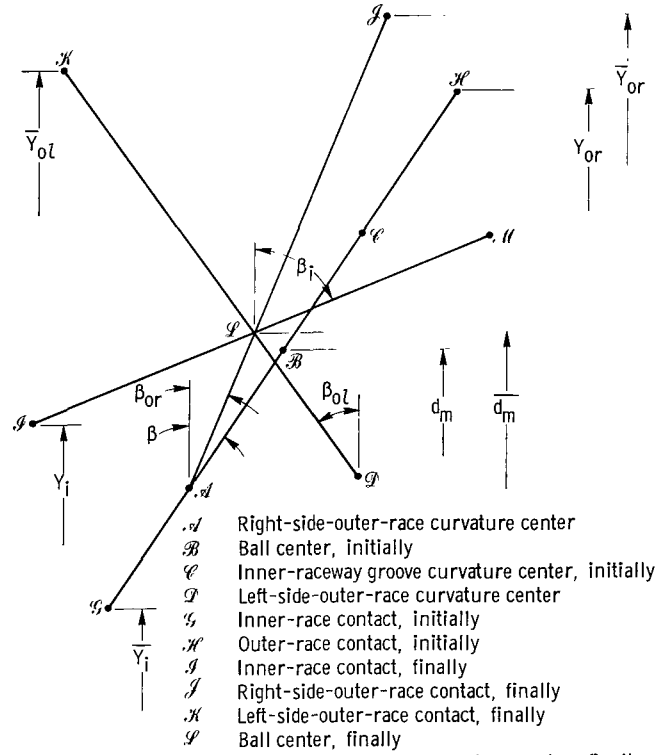

- $\mathscr{A}$ Right-side-outer-race curvature center
- $\mathscr{B}$ Ball center, initially
- $\mathscr{C}$ Inner-raceway groove curvature center, initially
- $\mathscr{D}$ Left-side-outer-race curvature center
- $\mathscr{G}$ Inner-race contact, initially
- $\mathscr{H}$ Outer-race contact, initially
- $\mathscr{I}$ Inner-race contact, finally
- $\mathscr{J}$ Right-side-outer-race contact, finally
- $\mathscr{K}$ Left-side-outer-race contact, finally
- $\mathscr{L}$ Ball center, finally
- $\mathscr{M}$ Inner-raceway groove curvature center, finally

Figure 7. - Position of ball and raceway groove curvature centers and contacts with and without centrifugal force acting on ball.

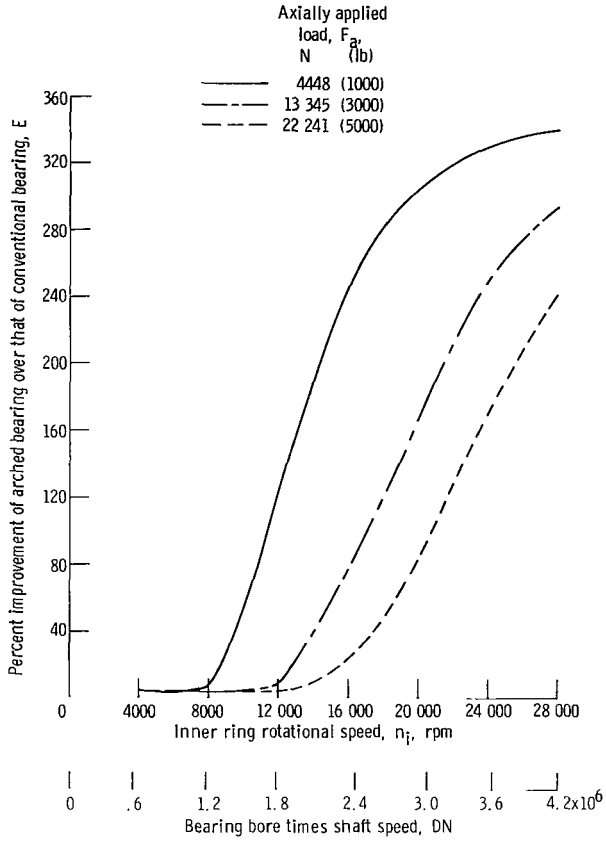

Figure 8. - Effect of speed on percent improvement of arched bearing (arching, 0.127 mm; 0.005 in.) compared to that of conventional bearing (zero arching) for various axially applied loads.

"The aeronautical and space activities of the United States shall be conducted so as to contribute . . . to the expansion of human knowledge of phenomena in the atmosphere and space. The Administration shall provide for the widest practicable and appropriate dissemination of information concerning its activities and the results thereof."

— NATIONAL AERONAUTICS AND SPACE ACT OF 1958

NASA SCIENTIFIC AND TECHNICAL PUBLICATIONS

TECHNICAL REPORTS: Scientific and technical information considered important, complete, and a lasting contribution to existing knowledge.

TECHNICAL NOTES: Information less broad in scope but nevertheless of importance as a contribution to existing knowledge.

TECHNICAL MEMORANDUMS: Information receiving limited distribution because of preliminary data, security classification, or other reasons.

CONTRACTOR REPORTS: Scientific and technical information generated under a NASA contract or grant and considered an important contribution to existing knowledge.

TECHNICAL TRANSLATIONS: Information published in a foreign language considered to merit NASA distribution in English.

SPECIAL PUBLICATIONS: Information derived from or of value to NASA activities. Publications include conference proceedings, monographs, data compilations, handbooks, sourcebooks, and special bibliographies.

TECHNOLOGY UTILIZATION PUBLICATIONS: Information on technology used by NASA that may be of particular interest in commercial and other non-aerospace applications. Publications include Tech Briefs, Technology Utilization Reports and Technology Surveys.

Details on the availability of these publications may be obtained from:

SCIENTIFIC AND TECHNICAL INFORMATION OFFICE

NATIONAL AERONAUTICS AND SPACE ADMINISTRATION

Washington, D.C. 20546